

## **Sediment transport to the deep canyons and open-slope of the western Gulf of Lions during the 2006 intense cascading and open-sea convection period**

A. Palanques<sup>a,\*</sup>, P. Puig<sup>a</sup>, X. Durrieu de Madron<sup>b</sup>, A. Sanchez-Vidal<sup>c</sup>, C. Pasqual<sup>c</sup>, J. Martín<sup>a</sup>,  
A. Calafat<sup>c</sup>, S. Heusner<sup>b</sup>, M. Canals<sup>c</sup>

<sup>a</sup> Institut de Ciències del Mar (CSIC), Passeig Marítim de la Barceloneta, 37-49. E-08003  
Barcelona, Spain.

<sup>b</sup> CEFREM, CNRS, UMR 5110, University of Perpignan, 52, Avenue Villeneuve, 66860  
Perpignan cedex, France.

<sup>c</sup> GRC Geociències Marines, Dept. d'Estratigrafia, Paleontologia i Geociències Marines,  
Universitat de Barcelona, E-08028, Barcelona, Spain.

\* Corresponding author. Tel.: 34 93 2309500; email [albertp@icm.csic.es](mailto:albertp@icm.csic.es).

### **ABSTRACT**

An array of mooring lines deployed between 300 and 1900 m depth along the Lacaze-Duthiers and Cap de Creus canyons and in the adjacent southern open slope was used to study the water and sediment transport on the western Gulf of Lions margin during the 2006 intense cascading period. Deep-reaching cascading pulses occurred in early January, in late January and from early March to mid-April. Dense water and sediment transport to the deep environments occurred not only through submarine canyons, but also along the southern open slope. During the deep cascading pulses, temporary upper and mid-canyon and open slope deposits were an important source of sediment to the deep margin. Significant sediment

transport events at the canyon head only occurred in early January because of higher sediment availability on the shelf after the stratified and calm season, and in late February because of the interaction of dense shelf water cascading with a strong E-SE storm. During the January deep cascading pulses, increases in suspended sediment concentration within the canyon were greater and earlier at 1000 m depth than at 300 m depth, whereas during the March-April deep cascading pulses sediment concentration only increased below 300 m depth, indicating resuspension and redistribution of sediments previously deposited at upper and mid-canyon depths. Deeper than 1000 m depth, net fluxes show that most of the suspended sediment left the canyon and flowed along the southern open slope towards the Catalan margin, whereas a small part flowed down-canyon and was exported basinward. Additionally, on the mid- and lower continental slope there was an increase in the near-bottom currents induced by deep open-sea convection processes and the propagation of eddies. This, combined with the arrival of deep cascading pulses, also generated moderate suspended sediment transport events in the deeper slope regions.

**Keywords:** sediment transport; submarine canyon; Gulf of Lions; dense shelf water cascading; open-sea convection; deep slope; deep sea

## 1. INTRODUCTION

Off-shelf sediment exports depend on the balance between sediment inputs, energy of hydrodynamic processes, shelf and slope morphology, and sediment instability (McCave, 1972; Milliman and Syvitski, 1992; Nittrouer and Wright, 1994). Off-shelf sediment transport can increase drastically during high-energy events such as storms or river floods (Monaco et al., 1990; Walsh and Nittrouer, 1999; Ogston et al., 2000; Puig et al., 2004a; Palanques et al.,

2005; Ulses et al., 2008a; Palanques et al., 2008; 2011, Martín et al., 2011). However, the specific mechanisms generating off-shelf and downslope transport pulses have not always been well identified. In some cases, sediment transport can be associated with processes such as sediment gravity flows (Paull et al., 2003; Khripounoff et al., 2003; Puig et al., 2003, 2004a; Xu et al., 2004) along-slope instabilities (Durrieu de Madron et al., 1999) and breaking of internal waves (Gardner et al., 1989; Puig et al., 2004b). Recently, dense shelf water cascading (DSWC) has also been identified as a mechanism that can generate high sediment fluxes in submarine canyons (Palanques et al., 2006; Heussner et al., 2006; Canals et al., 2006). Dense shelf water flow can transport shelf particles and erode and reshape the seafloor, increasing suspended and bed load across the shelf and slope. Erosional bedforms in some slope environments, such as sediment waves, erosional scours, furrows, and comet marks, have been attributed to dense bottom water flow (Canals et al., 2006; Trincardi et al., 2007; Davey and Jacobs, 2007; De Santis et al., 2007; Puig et al., 2008).

Cascading of dense water formed on the continental shelves throughout the world is an important mechanism for the ventilation of intermediate and deep waters in the oceans (see Ivanov et al., 2004 for a synthesis). The resulting flows cause an irreversible transfer of dissolved and particulate matter from the shelf to the deep ocean, playing an important role in biogeochemical cycles by removing phytoplankton and particulate and dissolved organic matter from productive areas and sequestering carbon (Hill et al., 1998, Niemann et al., 2004; Canals et al., 2006).

The magnitude of the downslope current induced by cascading depends on the density difference between the dense water plume and the ambient waters and on the slope angle, but is also significantly enhanced by the presence of submarine canyons, which steer the dense

overflows downslope (Darelius, 2008; Wahlin et al., 2008, Allen and Durrieu de Madron, 2009). DSWC in the Gulf of Lions (GoL) canyon heads has been extensively studied recently (Palanques et al., 2006; Puig et al., 2008; Ogston et al., 2008; Ribó et al., 2011). However, studies of dense shelf water spreading down and along the slope are scarce (e.g., Fer et al., 2003), and the effects of this bottom flow on deep-slope sediment transport are largely unknown. This paper aims to study the spreading of dense shelf water flow and its effects on sediment transport across and along the continental margin, both in submarine canyons and on the open slope at the southwestern end of the GoL, based on observations collected from October 2005 to October 2006. It also considers the interactions of DSWC and associated sediment load with open-sea convection on the continental rise.

## **2. GENERAL SETTING**

### **2.1. Study Area**

The GoL is a river-dominated, crescent-shaped continental margin located in the northwestern Mediterranean (Fig. 1). It is bounded to the southwest by the Cap de Creus promontory, where the shelf narrows to 2.6 kilometres, and to the northeast by Cap Croisette. Its continental slope is incised by numerous submarine canyons, which make it the most densely canyoned margin segment in the entire Mediterranean Sea. The hydrodynamics of the GoL is essentially driven by the general geostrophic circulation flowing cyclonically along the slope (the Northern Current), the various wind regimes and the fresh water discharge from rivers (Millot, 1990). The Northern Current is part of the cyclonic circulation of the Western Mediterranean Basin. The core of this current is several hundred metres thick and primarily composed of Atlantic Water (AW, upper 150 m) and Levantine Intermediate Water (LIW)

deeper below. It forms a density front that separates the coastal water from the more saline open seawater, constraining the shelf circulation and therefore influencing shelf-slope exchanges. The eastern flowing extension of the permanent circulation in the southern part of the GoL forms a cyclonic gyre that embeds the open ocean convection region (MEDOC group, 1970; Marshall and Schott, 1999)

Northwesterly (Tramontane) and northerly (Mistral) winds, which are constrained by the orography after the GoL, are very frequent and persistent (up to one month). Because of a reduced fetch, they both generate relatively small waves (significant wave height  $<2$  m, peak period  $<6$  s) on the inner shelf. These cold, dry winds have a substantial cooling effect in winter and are responsible for dense water formation. Conversely, southeasterly and easterly marine wind events are rare and brief (typically less than three days) and can generate major storms mainly in autumn and in winter. They are associated with large swells and a significant rise in the sea level on the coast as a consequence of shoreward water transport and low atmospheric pressure during these events, which induce downwelling in the western sector of the GoL (Palanques et al., 2006; Ulses et al., 2008c). Most of the fresh water discharge in the GoL originates from the Rhone River in the northeastern part of the shelf. However, several small rivers discharging along the GoL coast (Hérault, Orb, Aude, Agly, Têt and Tech) can also sporadically reach significant water discharges (Palanques et al., 2006; Bourrin and Durrieu de Madron, 2006). The highest river discharge periods are primarily found in spring and fall.

## **2.2 Formation of dense waters in the Gulf of Lions**

The GoL is a site of dense water formation owing to the effect of strong and persistent northern winds (Mistral and Tramontane). The formation occurs at two distinct locations: the shallow inner shelf (Dufau Julliand et al., 2004; Durrieu de Madron, 2005; Ulses et al., 2008b) and the deep basin (MEDOC Group, 1970; Schott and Leaman, 1991). The process occurring in the basin is characterized by wind-induced open-sea vertical convection that causes mixing of surface water with warmer but saltier LIW and deepening of the mixed layer, which reaches the seabed (>2000 m depth) in some years (Schott et al., 1996). On the shelf, despite the local river fresh water discharges, the intense wind-induced evaporation and cooling produce cold dense water that spreads mostly cyclonically along the continental shelf and is funnelled towards the narrowing southwestern shelf end, where it is constrained against the Cap de Creus promontory. The dense shelf water eventually overflows the shelf and cascades down the slope, especially through the southernmost canyons, until it reaches its hydrostatic equilibrium level. This off-shelf transport can be enhanced by concurrent E-SE storms that generate downwelling of dense shelf water (Palanques et al., 2006; 2008; Ulses et al., 2008c; Ribó et al., 2011).

The quantity of dense water formed over, and exported from, the shelf depends on the atmospheric conditions (Guarracino et al., 2005; Hermann et al., 2008). During cold dry winters most of the dense water formed over the shelf cascades to the deep basin (Palanques et al., 2009), whereas during mild winters dense water is mainly consumed by mixing with lighter ambient water, and only a small quantity escapes the shelf. Sediment erosion by intense dense shelf water flow has been observed on the shelf (Bourrin et al., 2008) and at the shelf edge (Ogston et al., 2008). The overflowing and cascading of this dense shelf water on the slope during the coldest years constitute a major mechanism of water and particulate matter transfer from the shelf to the deep slope (Canals et al., 2006; Heussner et al., 2006;

Palanques et al., 2009). The frequency of the severe events is difficult to anticipate. Béthoux et al. (2002) estimated, from the appearance of deep water anomalies in the deep basin since the 1960s, a sub-decadal recurrence for major cascading events. The long-term monitoring taking place since 1993 in the Lacaze-Duthiers Canyon (Fig. 2) shows that three extreme cascading events reaching at least 1000 m depth occurred in 1999, 2005 and 2006 in the GoL. During the 1999 and 2005 events, Dufau-Julliand et al. (2004) and Ulses et al. (2008b) estimated that the volume of dense shelf water exported from the GoL shelf represented at least the equivalent of the shelf water volume; this water reached the deep basin and contributed, together with the open-sea deep water formation, to the renewal of the Deep Western Mediterranean Water (Béthoux et al., 2002; Canals et al., 2006).

### **3. MATERIALS AND METHODS**

#### **3.1 Current meter data**

Near-bottom current, temperature and suspended sediment concentration in two submarine canyons, namely the Lacaze-Duthiers Canyon (LDC) and the Cap de Creus Canyon (CCC), and on the adjacent southern open slope (SOS) at the southwestern end of the GoL were studied by deploying nine moorings across the slope between 300 and 1900 m depth (Fig. 1). The moorings were deployed at 300, 1000 and 1500 m depth in the thalweg of both canyons and at their confluence at around 1900 m depth. Moorings on the SOS were deployed at 1000 and 1900 m depth. One Aanderaa RCM9/11 current meter equipped with temperature, conductivity and turbidity sensors was installed 5 m above bottom on each of these moorings. The current meter sampling interval was set to 30 minutes. The turbidity

sensor ranges were 0-100 Formazine Turbidity Units (FTU) at the canyon head sites (300 m) and 0-20 FTU at the other sites. The total recording period lasted from October 2005 to October 2006, and was divided into two consecutive deployments (mid-October 2005 to mid-April 2006, and mid-April 2006 to late October 2006). Owing to current meter failures, no hydrodynamical and hydrological data were recovered for the 1500 m mooring in the LDC and for the second deployment in the CCC at 1500 m and on the SOS at 1900 m.

Temperature and conductivity sensors were calibrated using contemporary CTD measurements collected during the deployment and recovery cruises (October 2005, April 2006 and October 2006). The conductivity signal had biofouling problems and was not considered. At some sites turbidity data showed a progressive increase in the signal background level at the end of the recording periods, also because of biofouling. The signals during these periods were corrected by removing the increasing trend. Turbidity values, recorded in FTU (Formazine Turbidity Unit), were converted into estimates of suspended sediment concentration (SSC), following the general calibration curves for the northwestern Mediterranean presented in Guillén et al. (2000):

- 1) For  $FTU > 0.2$ :  $SSC = 1.74 \times FTU - 1.32$  ( $N = 133, r^2 = 0.99$ ).
- 2) For  $FTU < 0.2$ :  $SSC = 0.79 \times FTU + 0.18$  ( $N = 159, r^2 = 0.61$ ).

### **3.2 Estimate of horizontal suspended sediment fluxes**

Instantaneous and net suspended sediment fluxes were calculated for each mooring site. Instantaneous sediment fluxes were obtained by multiplying the 30-min burst-averaged current speed by the instantaneous SSC measurement recorded every 30 min. Because of the

general anisotropy of the currents, we considered components along and across the local isobaths for moorings located on the open slope; for moorings located in canyons the along-canyon direction corresponds to that of the thalweg and the across canyon direction to the perpendicular of the thalweg. The integration of the instantaneous fluxes for the duration of the deployments yields the cumulated across- and along-isobath suspended-sediment fluxes. Instantaneous fluxes for both current components averaged over time gave the net across- and along-canyon suspended-sediment fluxes. From the resultant vector of those flux components, the estimated magnitude of the net horizontal flux of suspended sediment and the flux direction at each site were obtained.

### **3.3 Forcing conditions**

River water discharges to the GoL (Rhône, Hérault, Orb, Aude, Agly, Têt and Tech rivers) were measured by gauging stations close to the river mouths and supplied by the “Compagnie Nationale du Rhone” and the “Banque HYDRO” of the French Ministry of Environment. Wind speed and ocean-atmosphere heat fluxes averaged over the GoL were obtained from Météo-France weather model outputs. Significant wave height was measured by a wave buoy offshore of Sète (data from CANDHIS data bank). Gaps in the buoy time series were filled with the wave model outputs from the WW3 (WaveWatch 3) model forced by the winds and atmospheric pressure from the Meteo-France weather model.

## **4. RESULTS**

### **4.1 River discharge and wave climate**

Water discharges of selected rivers flowing into the GoL during the deployment period are shown in Figure 3. The Rhone River discharge was relatively low ( $<2000 \text{ m}^3 \text{ s}^{-1}$ ) until late February 2006 and increased in spring, reaching  $4050 \text{ m}^3 \text{ s}^{-1}$  on 12 April 2006. Most of the time, the Rhone River discharge was more than one order of magnitude higher than that of the other GoL rivers. Significant increases in the water discharge of the minor GoL Rivers occurred only in mid-November and late January, particularly in those flowing from the Massif Central (up to  $1000 \text{ m}^3 \text{ s}^{-1}$  on 30 January for the Aude, Hérault and Orb Rivers).

Waves recorded offshore of Sète (Fig. 4) showed moderate storms with  $H_s$  between 3.0 and 4.3 m occurring in early December, mid-January, mid-February and October, and a major southeastern storm with  $H_s$  reaching 5.3 m in late January. Frequent northern wind episodes reaching 14 to  $20 \text{ m s}^{-1}$  prevailed between early November 2005 and mid-March 2006 and induced large heat flux losses ( $>400 \text{ W m}^{-2}$ ) (Fig. 4).

#### **4.2 Near-bottom temperature**

In situ near-bottom temperature maintained relatively constant values above  $13.10 \text{ }^\circ\text{C}$  at most mooring sites from October to late December 2005 (Fig. 5). Between late December 2005 and April 2006 negative anomalies of different intensity and duration were recorded from 300 to 1900 m depth both in the submarine canyons and on the open slope. The strongest negative anomalies were recorded at the CCC 300 m site, where continuous temperature drops occurred during this period of time.

The intensity and the numbers of days of the temperature drops decreased with depth. At the CCC 300 site the greatest drops occurred in January, when temperature decreased to

11.08 °C (–2.20 °C). At the other sites, the mid-March to April 2006 drops were sharper than the January ones. During these drops, the temperature at 1000 m depth decreased to 11.99 °C, 12.22 °C and 12.40 °C at the CCC, LDC and SOS sites, respectively, so the drops were sharper in the CCC (up to –1.25 °C) than in the LDC and on the SOS (up to –1.02 °C and –0.81 °C respectively). At CCC 1500 the temperature fell to 12.61 °C (–0.57 °C) from mid-March to April, and at SOS 1900 and CCC 1900 it fell to 12.92 °C and 13.07 °C, respectively, in the same period (Fig. 5), so the temperature drops were higher on the SOS (up to –0.28 °C) than at the deep end of the CCC (up to –0.13 °C). Between May and October 2006 temperature increased progressively at the canyon heads (CCC 300 and LDC 300), whereas below 300 m it maintained fairly constant values.

#### **4.3. Near-bottom currents**

The near-bottom current time series (Fig. 5) showed great speed fluctuations mainly from January to April 2006 and many of the current peaks occurred simultaneous with the temperature drops described in the previous section and also shown in Figure 5. In the submarine canyons, current speeds peaked at 95 cm s<sup>-1</sup> at CCC 300 and at 73 cm s<sup>-1</sup> at LDC 300 and CCC 1000 in early January, whereas at LDC 1000 near-bottom currents only increased by up to 40 cm s<sup>-1</sup> in March. On the open slope, current speed at SOS 1000 increased to 40-54 cm s<sup>-1</sup> very often during the January-April period, with a peak in early January. At 1500 and 1900 m depths, repetitive current speed increases of 20-34 cm s<sup>-1</sup> were recorded both in the Cap de Creus submarine canyon and on the open slope from January to May-July 2006 (Fig. 5).

At the canyon heads (CCC 300 and LDC 300), currents were mainly oriented down-canyon (Fig. 6). At CCC 1000 and LDC 1000, currents were down-canyon when temperature drops occurred but most of the time, without temperature drops, the current was fluctuating up- and down-canyon. As a result, the progressive vectors of these sites show the lowest down-canyon displacements with across-canyon shifts (Fig. 7). At SOS 1000, the current was mainly oriented along-slope and southward. At CCC 1500, CCC 1900 and SOS 1900 the current direction was more scattered (Fig. 6), though with a NE-SW trend, and dominated by mesoscale rotating motions with periods of 3 to 15 days.

#### **4.4. Near-bottom suspended sediment concentration**

Time series of near-bottom SSC showed several peaks in the CCC and on the SOS, particularly in January and from March to April (Fig. 8). The highest SSC values were found at CCC 300 and CCC 1000. In the LDC, no significant SSC peaks were recorded.

In early January, SSC peaks reached  $37 \text{ mg l}^{-1}$  at CCC 300, more than  $39 \text{ mg l}^{-1}$  at CCC 1000 (i.e., turbidity above the sensor range), and  $14 \text{ mg l}^{-1}$  and  $8 \text{ mg l}^{-1}$  at CCC 1500 and CCC 1900, respectively. On the open slope, the strongest SSC peak was of  $23 \text{ mg l}^{-1}$  at the SOS 1000 site and only some small peak (of about  $2 \text{ mg l}^{-1}$ ) occurred at SOS 1900 in early January.

In late January, the strongest SSC peak ( $140 \text{ mg l}^{-1}$ ) was recorded at CCC 300 and peaks of up to  $37 \text{ mg l}^{-1}$  were recorded at CCC 1000, whereas SSC did not increase at the deeper canyon sites. On the open slope, only a small peak of  $4 \text{ mg l}^{-1}$  occurred at SOS 1000

and small peaks ranging between 3 and 4 mg l<sup>-1</sup> were recorded at SOS 1900 in late January and also in early February (Fig. 8).

Other significant SSC increases also occurred in late March and early April, not at CCC 300 but at CCC 1000 and SOS 1000, with several peaks of between 5 and 10 mg l<sup>-1</sup> and one major peak of 22 mg l<sup>-1</sup> at CCC 1000. At greater depths, some small SSC increases were observed at CCC 1500 and CCC 1900 (1-2 mg l<sup>-1</sup>) and more significant peaks (up to 6 mg l<sup>-1</sup>) at SOS 1900 in late March and early April.

#### **4.5 Suspended sediment transport**

The temporal evolution of instantaneous suspended sediment fluxes varied more than 4 orders of magnitude, between 1 x 10<sup>-3</sup> g m<sup>-2</sup> s<sup>-1</sup> at the deeper sites and more than 94 g m<sup>-2</sup> s<sup>-1</sup> at CCC 300 in late January (data not shown).

The cumulative suspended sediment transport showed a predominant down-canyon component at CCC 300 and CCC 1000, whereas at CCC 1500 and CCC 1900 the across-canyon (along-slope) cumulative flux was higher than the along-canyon cumulative flux (Fig. 9). Within the CCC, the maximum cumulative sediment transport took place in early January, when a dominant down-canyon sediment transport affected all the canyon sites from 300 to 1900 m depth. The late January event produced lower cumulative transport in spite of the higher instantaneous SSF. In late March, down-canyon cumulative sediment transport only showed an increasing event at CCC 1000. On the open slope, a predominant along-slope suspended sediment transport towards the SW was observed (Fig. 9).

These trends were also shown by the net suspended sediment fluxes during the cascading season (January to April). Higher net fluxes were recorded in the Cap de Creus canyon at the 300 and 1000 depth sites (668 and 310 mg m<sup>-2</sup> s<sup>-1</sup>, respectively), with a down-canyon resultant vector. On the open slope and at the canyon sites deeper than 1000 m, the direction of the resultant vector of the net flux was along isobaths and across-canyon, respectively. Net fluxes suggest a sediment transport overflowing the canyon beyond 1000 m depth with a dominant along-slope component towards the south (Fig. 10).

## **4.6. Deep cascading pulses**

### *4.6.1. Early January deep cascading pulses*

During most of this event, several drops in temperature down to 11.36 °C occurred at CCC 300, along with simultaneous increases in current velocity reaching down-canyon speeds higher than 60 cm s<sup>-1</sup> and a peak of 95 cm s<sup>-1</sup> (Fig. 11). Moderate SSC increases (1.2-6.7 mg l<sup>-1</sup>) took place from the beginning of this pulse (on 3 January) and for more than three days, until a strong SSC (37 mg l<sup>-1</sup>) and sediment transport peak (27 g m<sup>-2</sup> s<sup>-1</sup>) occurred 40 hours after reaching maximum current speeds around 90 cm s<sup>-1</sup>. A different behaviour was observed at CCC 1000, where SSC increased slightly (~ 5 mg l<sup>-1</sup>) when the cascading pulse began to reach this site, 60 h later than reaching CCC 300, and peaked to values >38 mg l<sup>-1</sup> just when current speed reached maximum values (70 cm s<sup>-1</sup>), maintaining these high concentrations for more than 10 hours (Fig. 11). After this peak, there were five SSC peaks, two of them over 38 mg l<sup>-1</sup>, which also coincided with current speed increases and temperature drops. On the LDC no significant SSC peaks occurred during these DSWC pulses.

On the open slope, the dense shelf water plume arrived at SOS 1000 75 h later than at CCC 300; SSC increased immediately (up to  $23 \text{ mg l}^{-1}$ ) during the first strong current speed peak  $>50 \text{ cm s}^{-1}$  and the temperature fell slightly to  $12.7 \text{ }^{\circ}\text{C}$ . After this first SSC peak, there were four more also coinciding with current speed increases and temperature drops. At CCC 1500 m there was a significant SSC peak ( $14 \text{ mg l}^{-1}$ ) during the first temperature drop to  $12.8 \text{ }^{\circ}\text{C}$ , coinciding with a small current speed peak of  $20 \text{ cm s}^{-1}$  (Fig. 11). At CCC 1900, small SSC increases occurred along with very small temperature drops (in the range of the temperature resolution of  $0.02 \text{ }^{\circ}\text{C}$ ) and current speed peaks reaching  $33 \text{ cm s}^{-1}$  (Fig. 11). At SOS 1900 this first deep cascading pulse did not produce any SSC increase linked to a temperature decrease, but SSC increased later, linked to a current speed increase not coinciding with the arrival of the deep cascading pulse.

#### *4.6.2. Late January deep cascading pulses*

On 26 January 2006, another deep cascading pulse reached CCC 1000, generating a sudden temperature drop to  $12.1 \text{ }^{\circ}\text{C}$ , a current speed increase to  $58 \text{ cm s}^{-1}$  and a SSC peak of  $35 \text{ mg l}^{-1}$  (Fig. 12). This pulse was also recorded in the LDC, but there temperature decreased to  $12.5 \text{ }^{\circ}\text{C}$  and SSC only increased to  $5.5 \text{ mg l}^{-1}$ . Another deep cascading pulse reached CCC 1000 on 29 January, showing similar characteristics to the previous one. None of these SSC peaks were recorded at CCC 300, where current speed and SSC started to increase progressively on 28 January at the time when a major southwestern storm affected the GoL (Fig. 12). This storm had its peak on 28 January and lasted three days. Two days after the peak of the storm on 30 January, a sharp SSC increase reaching  $140 \text{ mg l}^{-1}$  took place at CCC 300, associated with a temperature drop ( $11.1 \text{ }^{\circ}\text{C}$ ) and an increase in current speed. At the LDC 300 site SSC did not increase in late January. At SOS 1000 a small SSC increase of 4

mg l<sup>-1</sup> occurred simultaneously with a small temperature drop (Fig. 12). No significant SSC peaks were recorded at CCC 1500 and CCC 1900, whereas some small SSC peaks occurred at SOS 1900 but did not coincide with cascading pulses.

#### *4.6.3. March-April deep cascading*

Deep cascading pulses were observed again from mid-March to mid-April. During this period of time, cascading did not produce any significant SSC peaks at CCC 300, whereas several cascading pulses reached CCC 1000 and SOS 1000, generating moderate SSC peaks of 4 to 22 mg l<sup>-1</sup> (Fig. 13). These peaks were associated with current speed increases to 50 and 47 cm s<sup>-1</sup> and temperature drops to 12.07 °C and 12.51 °C at CCC 1000 and SOS 1000, respectively. In the LDC, turbidity sensors were affected by fouling and only some small peaks (6 mg l<sup>-1</sup>) associated with DSWC were clearly recorded at LDC 1000 in early March (data not shown). Some of these deep cascading pulses were recorded at CCC 1500, CCC 1900 and SOS 1900, but they only produced some small temperature drops that were not linked to current speed or SSC increases. Some isolated SSC peaks occurred at the 1900 m depth sites, showing higher concentrations (up to 4 mg l<sup>-1</sup>) at SOS 1900, but not coinciding with any deep cascading pulse.

## **5. DISCUSSION**

### **5.1. Multistep sediment transport**

The analysis of the recorded sediment transport events gives information about the effects and interactions of the various processes affecting the downcanyon and deep slope

sediment transport in the western GoL. The recorded data show that cascading occurred at the canyon head very frequently from December 2005 to May 2006, but it only reached the deeper sites during a few pulses occurring in early and late January and from mid-March to mid-April.

At the canyon heads, the frequent current speed increases not associated to any SSC increase indicate that the erodible sediment is very limited because the strong currents induced by DSWC and major E and SE storms deplete it quite often. This was also observed during the 2005 winter by Puig et al., (2008), Ogston et al. (2008), and DeGeest et al. (2008). In winter 2006 the recorded data indicate that the amount of sediment that could be resuspended by DSWC at the canyon head sites was limited, and the SSC peaks at CCC 3000 were caused by advection of sediment previously resuspended on the shelf. In early January 2006, when the dense shelf water plume reached the CCC canyon head, current speeds increased up to  $90 \text{ cm s}^{-1}$  but SSC did not peak until a few days later (Fig.11). Therefore this SSC peak was not caused by winnowing of erodible sediment at the canyon head but by resuspension and advection of erodible shelf sediment previously accumulated in summer and autumn.

Also, the strong SSC increase occurring at the canyon head on 30 January was not generated by local resuspension at this site but by the off-shelf advection of shelf sediment resuspended by a major E-SE storm. This sediment load reached the canyon head two days after the peak of the storm and a few days after the late-January deep DSWC pulses, and it did not reach CCC 1000 (Fig. 12). The action of major E-SE storms flushing large amounts of shelf resuspended sediment through the CCC, by inducing downwelling and intensifying cascading, has also been evidenced in other extreme storms occurring in the area (Palanques

et al., 2006; 2008; Ribó et al., 2011). During the following deep DSWC pulses occurring from March to April, SSC did not increase at CCC 300 (Fig. 13) because erodible sediment from the shelf and the canyon head had been previously exhausted.

In absence of deep cascading pulses (>1000 m), the sediment transported by cascading and major E-SE storms is deposited just beyond the canyon head (400–700 m depth), where the dense water flow loses competence and unconsolidated muddy layers may be unconformably overlying sand or consolidated mud in a non-steady accumulation state (DeGeest et al., 2008). Given the low interannual recurrence of deep cascading pulses (see Fig. 3) with respect to the frequent events affecting the canyon head, the sediment deposits in the middle part of the canyon have a longer residence time than the shallower erodible sediment. When deep cascading pulses reach this temporary accumulation zone, the recorded data indicate that they resuspend and transport the unconsolidated sediment until the available erodible sediment is depleted. If there is no sediment available to be resuspended and transported from the shelf and/or the canyon head, the increase in SSC and sediment transport during a deep cascading pulse begins from this temporary accumulation zone, beyond the canyon head. This was observed at the beginning of the January deep cascading pulses and during the mid-March to mid-April deep cascading pulses (Figs. 11, 12 and 13).

During the January deep DSWC pulses, the first SSC peaks at CCC 1000 and SOS 1000 occurred one to three days before any SSC increase at CCC 300 and took place as soon as the deep cascading pulse increased current speed (Figs. 11 and 12). During the March-April deep DSWC pulses, SSC peaks at the 1000 m depth sites (mainly CCC 1000 and SOS 1000) were also produced from resuspension of these temporary deposits. Similar downcanyon increases in the suspended load from below the CCC head, associated with the

entrainment of sediment temporarily deposited in the upper canyon section, were also observed in the 2005 winter (Puig et al., 2008).

At 1000 m depth, both in the CCC and on the SOS, the sediment transport was stronger during the first deep cascading pulses in January than during the last pulses in March-April. This was a consequence of the higher current (Fig. 6) and sediment availability in January, than at the end of the cascading period, when probably most of the erodible sediment had already been winnowed. Puig et al. (2008) also observed a decrease in SSC with time due to winnowing and progressive exhaustion of the resuspendible sediments by cascading currents down to 750 m depth during the 2005 winter.

As a consequence of this progressive exhaustion of resuspendible sediments on the mid canyon temporary deposits, only the first deep DSWC pulses generated a significant SSC increase (up to  $14 \text{ mg l}^{-1}$ ) at CCC 1500 in early January (Fig. 11). This increase occurred some hours after the major SSC peak at CCC 1000 and coincided with temperature drops, but not with strong current peaks. This data indicates that the increase was produced by sediment resuspended at the mid canyon area and advected by cascading to CCC1500. Another small SSC peaks at CCC 1500 and CCC 1900 did not seem to be associated with the temperature drops caused by the deep DSWC pulses but with current speed increases presumably associated with dense water formation by open-sea convection. Deep DSWC pulses did not generate any significant SSC increase at the SOS 1900 site (Figs. 11 and 13)

Integrating all the 2006 cascading season, net suspended sediment fluxes indicates that most of the sediment transport by deep DSWC overflows the canyon beyond the CCC 1000 and flows with a dominant alongslope component towards the south (Fig. 10). This is in

accordance with the presence of furrows in the CCC down to about 1400 m depth (Canals et al., 2006; Lastras et al., 2007; Puig et al., 2008), where the canyon section widens and the height of the southern flank drops. These topographic factors added to the reduction of the density excess of the dense water plume may produce a deceleration of the bottom flow, losing part of its erosive capability and coarse sediment load and leaving the canyon confinement. However, the net suspended sediment flux, the slope morphology (Fig 10) and the still strong currents at SOS 1000 suggest that the cascading flows contour the open slope beyond the southern canyon wall between about 700 and 1300 m depth, transporting its sediment load and maintaining a steep topography on the mid slope towards the south. Outside the strong confinement of the canyon walls and the contouring at the mid slope, the sediment advected by dense shelf water to the deep slope was dispersed by the currents associated with open-sea convection, giving net suspended sediment fluxes flowing along-isobaths.

Therefore, there is a multi-step sediment transport from the shelf to the upper slope by storms and DSWC, from the upper slope to the deep slope by deep cascading pulses, and from the deep slope to the basin by open-sea convection. This multistep sediment transport is consistent with the collection of resuspended sediment and degraded organic matter by near-bottom sediment traps in the mid-canyon and in the basin during the 2005 deep cascading events (Puig et al., 2008; Tesi et al., 2009; Palanques et al., 2009). The analysis of the material collected by sediment traps in the 2006 winter (placed on the same mooring lines as those deployed for this study) shows a decrease in the major organic components (organic carbon and opal) and an increase in the coarse (sand) fraction mainly at the canyon head and the 1000 m depth sites (Sanchez-Vidal et al., 2009; Pasqual et al., 2010).

## **5.2. Open-sea convection and its effect on sediment transport**

DSWC began in late December 2005 causing drops in temperature and sharp peaks in down-canyon current velocities and SSC at the canyon heads. This occurred almost simultaneously with increases in current speed, SSC and temperature at the deeper sites (CCC 1500, CCC 1900 and SOS 1900) because of the arrival of water slightly warmer than ambient waters (Figs. 5, 6 and 8). These changes in hydrologic and hydrodynamic conditions in the deep slope were related to open-sea convection that occurred concomitantly to dense shelf water formation. It is known that the same persistent cold and dry winds that form dense water on the shelf also cause open-sea convection in the GoL (Marschall and Schott, 1999, and references therein), generating a simultaneous triggering of offshore convection and shelf-water cascading in the region. When the open-sea convection reaches the sea floor, it forms new deep water that is slightly saltier and warmer than the ambient waters above the bottom, resulting from the mixing of LIW and WMDM (Font et al., 2007). Thus, the formation of warmer deep water at the deeper sites corresponded to the arrival of newly-formed deep water from the open-sea convection area.

On the deep slope of the GoL, open sea convection water is spread by deep eddies (both anticyclonic and cyclonic) that drift far away from the deep convection area. Most of these eddies first drift toward the southwest and later turn northeastward (Testor and Gascard, 2006). At CCC 1900 and SOS 1900, the current speed increased and current direction changed cyclically with the pass of eddies, indicating an intensification of meso-scale current activity due to convection (Figs. 6 and 7). Some current increases associated to open-sea convection induced small SSC increases by resuspension and/or lateral advection of deep slope sediment previously transported by cascading pulses. This can be observed at CCC

1500, CCC 1900 and SOS 1900, where some small SSC increases occurred during the strongest current peaks, not coinciding with temperature drops, and therefore associated with open sea dense water formation by convection (Figs. 11, 13 and 14). At CCC 1900, the sediment transport associated with these SSC increases was dominantly up- and down-canyon, whereas on the open slope at SOS 1900 it was mainly alongslope (towards the SW) and downslope (Fig. 14). The residual sediment transport at these two deep sites was primarily along isobaths (Fig. 10).

The capacity of the currents induced by open sea convection to resuspend and/or transport suspended sediment was also observed by Martín et al. (2010) in the Ligurian Sea, where new deep water was formed and reached about 2000 m depth during the same winter 2006 (Smith et al., 2008; Martín et al., 2010). Martín et al. (2010) recorded near-bottom downward particle flux increases (measured by sediment traps) of between one and two orders of magnitude, reaching values of up to  $9 \text{ g m}^{-2} \text{ d}^{-1}$ . These increases were associated with current speed peaks reaching values of between 25 and 38  $\text{cm s}^{-1}$ , which were induced by open-sea convection and were able to resuspend and relocate deep sediment. Likewise, in the deep slope of the GoL, the most significant SSC peaks shown in the present study were mainly caused by current peaks, also induced by open-sea convection and reaching values of between 18 and 34  $\text{cm s}^{-1}$  (Fig. 14). During the 2006 open sea convection period, near-bottom downward particle fluxes at CCC 1900 and SOS 1900 measured by sediment traps were between 1 and 5.7  $\text{g m}^{-2} \text{ d}^{-1}$  (Pascual et al., 2010), of a similar magnitude to those observed in the Ligurian Sea by Martín et al. (2010) during the same year.

## **6. CONCLUSIONS**

The set of mooring arrays deployed between October 2005 and November 2006 on the canyons and open slope of the western GoL provided a unique description of the strong hydrodynamic events and suspended sediment transport that occurred during the winter 2006. The overflow of dense shelf water and spreading down the deep slope was observed and tracked. Interactions with stormy events in the upper canyon and with open-sea convection in the deep slope were evidenced. In winter 2006, maximum sediment transport took place in the CCC, whereas no significant sediment transport events were recorded in the LDC, confirming the predominant role of the CCC in exporting shelf water and associated sediment to the slope.

The first cascading pulses each winter produce the off-shelf export of the erodible sediment available on the shelf after the calmer stratified season. In addition, shelf sediment resuspended by major E-SE storms can be massively exported downcanyon because of the DSWC intensification caused by storm-induced downwelling. DSWC and major E-SE storms transport shelf sediment usually to the upper-mid canyon area, where it accumulates temporarily. Less frequent deep cascading pulses resuspend and again transport the sediment from these temporary deposits. As erodible sediment of the shelf and the canyon head is frequently exhausted, during deep cascading pulses the increases in sediment transport are generated mainly from resuspension of these mid-canyon temporary deposits. Beyond the mid CCC, most of the suspended sediment transported by deep DSWC in winter 2006 left the canyon confinement and was transported along the southern open mid-slope, whereas a small part flowed down-canyon. The dense water plume overflowing the southern mid canyon wall flowed contouring the southern open mid-slope, following and probably maintaining a steep alongslope topography that extends towards the Catalan margin.

Although deep cascading pulses reached the deep margin, significant sediment transport events on the deep slope (CCC 1900 and SOS 1900) were mainly controlled by open sea convection that intensified current speed and eddies. Open-sea convection must be considered as a significant deep sediment transport process that is able to resuspend and transport bottom sediment, when it reaches the deep sea floor.

In summary, when deep cascading pulses occur in the GoL a multi-step sediment transport is observed: from the shelf to the upper slope by storms and DSWC, from the upper slope to the lower slope by deep cascading pulses; and finally, from the lower slope to further offshore by currents associated to open-sea convection. The interaction of these processes is important for the dispersal of water and sediment and associated particulate and dissolved chemical elements towards and throughout the NW Mediterranean deep basin.

**Acknowledgements.** We thank all participants, UTM technicians and crews of R/V Garcia del Cid and R/V Universitatis, for their help and dedication during the cruises. The research projects HERMES (GOCE-CT-2005-511234-1), HERMIONE (FP7-ENV-2008-1-226354), DOS MARES (CTM2007-66316-C02-01/MAR) and GRACCIE-CONSOLIDER (CSD2007-00067) supported this research. ASV, CP, AC and MC belong to CRG on Marine Geosciences, supported by grant 2009 SGR 1305 of the Generalitat de Catalunya. AP, PP and JM belong to CRG on Littoral and Oceanic Processes, supported by grant 2009 SGR 899 of the Generalitat de Catalunya

## **REFERENCES**

Allen S., Durrieu de Madron, H., 2009. A review of the role of submarine canyons in deep-

ocean exchange with the shelf. *Ocean Sciences* 6, 1-38.

Béthoux, J.P., Durrieu de Madron, X., Nyffeler, F., Tailliez, D., 2002. Deep water in the western Mediterranean: peculiar 1999 and 2000 characteristics, shelf formation hypothesis, variability since 1970 and geochemical inferences. *Journal of Marine Systems* 33-34, 117-131, doi:10.1016/S0924-7963(02)00055-6. 498

Bourrin F., Durrieu de Madron, X., 2006. Contribution to the study of coastal rivers and associated prodeltas to sediment supply in the Gulf of Lions (N-W Mediterranean Sea). *Vie & Milieu - Life & Environment* 56 (4), 1-8.

Bourrin, F., Durrieu de Madron, X., Heussner, S., Estournel, C., 2008. Impact of winter dense water formation on shelf sediment erosion (evidence from the Gulf of Lions, NW Mediterranean). *Continental Shelf Research* 28 (15), 1984-1999.

Canals, M., Puig, P., Durrieu de Madron, X., Heussner, S., Palanques, A., Fabres, J., 2006. Flushing submarine canyons. *Nature* 444, 354-357, doi:10.1038/nature05271. 506

Darelius, E., 2008. Topographic steering of dense overflows: Laboratory experiments with V-shaped ridges and canyons. *Deep-Sea Research I* 55, 1021– 1034.

Davey, F.J., Jacobs, S.S., 2007. Influence of submarine morphology on bottom water flow across the western Ross Sea continental margin. In Cooper, A.K., Raymond, C. R. et al. (Eds),

Online Proceedings of the 10th ISAES, USGS Open-File Report 2007-1047, Short Research Paper 067, 5 p.; doi: 10.3133/of2007-1047.srp067.

DeGeest, A.L., Mullenbach, B.L., Puig, P., Nittrouer, C.A., Drexler, T.M., Durrieu de Madron, X., Orange, D.L., 2008. Sediment accumulation in the western Gulf of Lions, France: the role of Cap de Creus Canyon in linking shelf and slope sediment dispersal systems. *Continental Shelf Research* 28, 2031–2047, doi:10.1016/j.csr.2008.02.008.

De Santis L., G. Brancolini, D. Accettella, A. Cova, A. Caburlotto, F. Donda, C. Pelos, F. Zgur, M. Presti (2007), New insights into submarine geomorphology and depositional processes along the George V Land continental slope and upper rise (East Antarctica). In Cooper, A.K., Raymond, C. R. et al. (Eds), *Online Proceedings of the 10th ISAES X, USGS Open-File Report 2007-1047, Extended Abstract 061, 5 p.*

Dufau-Julliand, C., Marsaleix, P., Petrenko, A., Dekeyser, I., 2004. Three-dimensional modeling of the Gulf of Lion's hydrodynamics (north-west Mediterranean) during January 1999 (MOOGLI3 Experiment) and late winter 1999: Western Mediterranean Intermediate Water's (WIW's) formation and its cascading over the shelf break. *Journal of Geophysical Research* 109, C11002, doi:10.1029/2003JC002019.

Durrieu de Madron, X., Radakovitch, O., Heussner, S., Loye-Pilot, M.D, Monaco, A., 1999. Role of the climatological and current variability on shelf-slope exchanges of particulate matter. Evidence from the Rhône continental margin (NW Mediterranean). *Deep-Sea*

Research I 46, 1513-1538.

Durrieu de Madron, X., Zervakis, V., Theocharis, A., Georgopoulos, D., 2005. Comments on “Cascades of dense water around the world ocean.” *Progress in Oceanography* 64: 83–90, doi:10.1016/j.pocean.2004.08.004.

Fer, I., Skogseth, R., Haugan, P.M., Jaccard, P., 2003. Observations of the Storfjorden overflow. *Deep-Sea Research I* 50, 1283–1303.

Font, J., Puig, P., Salat, J., Palanques, A., Emelianov, M., 2007. Sequence of hydrographic changes in the NW Mediterranean deep water due to the exceptional winter 2005. *Scientia Marina* 72, 339–346.

Gardner, W. D., 1989. Periodic resuspension in Baltimore canyon by focusing of internal waves, *Journal of Geophysical Research* 94, 18185– 18194.

Guarracino, M., Barnier, B., Marsaleix, P., Durrieu de Madron, X., Monaco, A., Escoubeyrou, K., Marty, J.-C., 2006, Transfer of particulate matter from the northwestern Mediterranean continental margin: Variability and controlling factors. *Journal of Marine Research* 64, 195–220.

Guillén, J., Palanques, A., Puig, P., Durrieu de Madron, X., Nyffeler, F., 2000. Field calibration of optical sensors for measuring suspended sediment concentration in the Western

Mediterranean. *Scientia Marina* 64 (4), 427–435.

Hermann, M., Estournel, C., Déqué, M., Marsaleix, P., Sevault, F., Somot, S., 2008. Dense water formation in the Gulf of Lions: Impact of atmospheric interannual variability and climate change. *Continental Shelf Research* 28 (15), 2092-2112.

Heussner, S., Durrieu de Madron, X., Calafat, A., Canals, M., Carbonne, J., Delsaut, N., Saragoni, G., 2006. Spatial and temporal variability of downward particle fluxes on a continental slope: Lessons from an 8-yr experiment in the Gulf of Lions (NW Mediterranean). *Marine Geology* 234, 63-92, doi:10.1016/j.margeo.2006.09.003.547

Hill, A.E., Souza, A.J., Jones, K.J., Simpson, H., Shapiro, G.I., McCandliss, R., Wilson, H., Leftley, J., 1998. The Malin cascade in winter 1996. *Journal of Marine Research* 56, 87–106,

Ivanov, V.V., Shapiro, G. I., Huthnance, J. M., Aleynik, D. L., Golovin, P. N., 2004. Cascades of dense water around the world ocean. *Progress in Oceanography* 60, 47 – 98.

Khripounoff, A., Vangriesheim, A., Babonneau, N., Crassous, P., Dennielou, B., Savoye, B., 2003. Direct observation of intense turbidity current activity in the Zaire submarine valley at 4000 m water depth. *Marine Geology* 194, 151-158.

Lastras, G., Canals, M., Urgeles, R., Amblas, D., Ivanov, M., Droz, L., Dennielou, B., Fabrès, J., Schoolmeester, T., Akhmetzhanov, A., Orange, D., Garcia-Gracia, A., 2007. A walk down

the Cap de Creus canyon, Northwestern Mediterranean Sea: Recent processes inferred from morphology and sediment bedforms. *Marine Geology* 246, 2-4, 176-192.

Marschall J., Schott, F., 1999. Open-ocean convection: observations, theory, and models. *Reviews of Geophysics* 37 (1), 1-64.

Martín, J., Miquel, J.C., Khripounoff, A., 2010. Impact of open sea deep convection on sediment remobilization in the western Mediterranean. *Geophysical Research Letters* 37, L13604, doi:10.1029/2010GL043704

McCave, I.N., 1972. Transport and escape of fine-grained sediment from shelf areas. In Swift, D.J.P., Duane, D. B., Pilkey, O. H. (Eds.), *Shelf Sediment Transport: Process and Pattern*. Van Nostrand Reinhold, New York, pp. 225-248.

MEDOC group., 1970. Observation of formation of deep water in the Mediterranean Sea, 1969. *Nature* 227, 1037-1040.

Milliman, J. D., Syvitski, J. P. M., 1992. Geomorphic/tectonic control of sediment discharge to the ocean: the importance of small mountainous rivers. *Journal of Geology* 100, 525–544.

Millot, C., Monaco, A., 1984. Deep intense currents and sedimentary transport in the northwestern Mediterranean Sea. *Geo-Marine Letters* 4, 13-17.

Monaco, A., Courp, T., Heussner, S., Carbonne, J., Fowler, S.W., Deniaux, B., 1990. Seasonality and composition of particulate fluxes during ECOMARGE-I western Gulf of Lions. *Continental Shelf Research* 9-11, 959-987.

Niemann H., Richter, C., Jonkers, H.M., Badran, M.I., 2004. Red Sea gravity currents cascade near-reef phytoplankton to the twilight Zone. *Marine Ecology Progress Series* 269, 91-99.

Nittrouer, C.A., Wright, L.D., 1994. Transport of particles across continental shelves. *Reviews of Geophysics* 32, 85-113.

Ogston, A. S., Cacchione, D. A., Sternberg, R. W., Kineke, G. C., 2000. Storm and river flood-driven sediment transport on the northern California continental shelf. *Continental Shelf Research* 20, 2141– 2162.

Ogston, A.S., Drexler, T.M., Puig, P., 2008. Sediment delivery, resuspension, and transport in two contrasting canyon environments in the southwest Gulf of Lions. *Continental Shelf Research* 28 (15), 2000-2016.

Palanques, A., El Khatab, M., Puig, P., Masqué, P., Sánchez-Cabeza, J. A., Isla, E., 2005. Downward particle fluxes in the Guadiaro submarine canyon depositional system (north-western Alboran Sea), a river flood dominated system. *Marine Geology* 220 (1-4), 23-40.

Palanques, A., Durrieu de Madron, X., Puig, P., Fabres, J., Guillén, J., Calafat, A., Canals, M.,

Heussner, S., Bonnin, J., 2006. Suspended sediment fluxes and transport processes in the Gulf of Lions submarine canyons. The role of storms and dense water cascading. *Marine Geology* 234, 43-61, doi:10.1016/j.margeo.2006.09.002583.

Palanques, A., Guillén, J., Puig, P., Durrieu de Madron, X., 2008. Storm-driven shelf-to-canyon suspended sediment transport at the southwestern end of the Gulf of Lions. *Continental Shelf Research* 28, 1947–1956.

Palanques, A., Puig, P., Latasa, M., Scharek, R., 2009. Deep sediment transport induced by storms and dense shelf water cascading in the northwestern Mediterranean basin. *Deep-Sea Research I*, 56, 425-434.

Pasqual, C., Sanchez-Vidal, A., Zúñiga, D., Calafat, A., Canals, M., Durrieu de Madron, X., Puig, P., Heussner, S., Palanques, A., Delsaut, N., 2010. Flux and composition of settling particles across the continental margin of the Gulf of Lion: the role of dense shelf water cascading. *Biogeosciences* 7, 217–231.

Paull, C.K., Ussler, W., Greene, H.G., Keaten, R., Mitts, P., Barry, J., 2003. Caught in the act: the 20 December 2001 gravity flow event in Monterey Canyon. *Geo-Marine Letters* 22, 227 – 232.

Puig, P., Palanques, A., Guillén, J., García-Ladona, E., 2000. Deep slope currents and suspended particle fluxes in and around the Foix submarine canyon (NW Mediterranean).

Deep-Sea Research 47, 343–366.

Puig, P., Ogston, A.S., Mullenbach, B.L., Nittrouer, C.A., Sternberg, R.W., 2003. Shelf-to-canyon sediment-transport processes on the Eel continental margin (northern California). *Marine Geology* 193, 129-149.

Puig, P., Ogston, A.S., Mullenbach, B.L., Nittrouer, C.A., Parsons, J.D., Sternberg, R.W., 2004a. Storm-induced sediment gravity flows at the head of the Eel submarine canyon, northern California margin. *Journal of Geophysical Research* 109 (C3), C03019.

Puig, P., Palanques, A., Guillén, J., El Khatab, M., 2004b. The role of internal waves in the generation of nepheloid layers in the northwestern Alboran slope: implications for continental margin shaping. *Journal of Geophysical Research* 109, C09011-11 pp.

Puig, P., Palanques, A., Orange, D.L., Lastras, G. and Canals, M., 2008. Dense shelf water cascades and sedimentary furrow formation in the Cap de Creus Canyon, northwestern Mediterranean Sea; *Continental Shelf Research*, 2017– 2030. doi:10.1016/j.csr.2008.05.002

Ribó, M., Puig, P., Palanques, A., Lo Iacono, C., 2011. Dense shelf water cascades in the Cap de Creus and Palamós submarine canyons during winters 2007 and 2008. *Marine Geology*.

Sanchez-Vidal, A., Pasqual, C., Kerherve, P., Heussner, S., Calafat, A., Palanques, A., Durrieu de Madron, X., Canals, M., Puig, P., 2009. Across margin export of organic matter by

cascading events traced by stable isotopes, northwestern Mediterranean Sea. *Limnology and Oceanography* 54, 1488–1500.

Schott, F., Leaman, K.D., 1991. Observations with Moored Acoustic Doppler Current Profilers in the Convection Regime in the Golfe du Lion. *Journal of Physical Oceanography* 21, 558-574.

Schott, F., Visbeck, M., Send, U., Fisher, J., Stramma, L., Dsaubies, Y., 1996. Observations of deep convection in the Gulf of Lions, Northwestern Mediterranean during the winter of 1991/92. *Journal of Physical Oceanography* 26, 505-524.

Smith, R. O., Bryden, H. L., Stansfield, K., 2008. Observations of new western Mediterranean deep water formation using Argo floats 2004–2006. *Ocean Sciences* 4, 133–149.

Tesi, T., Puig, P., Palanques A., Goñi, M.A., 2010. Lateral advection of organic matter in cascading-dominated submarine canyons. *Progress in Oceanography* 84, 185–203.

Testor, P., Gascard, J.C., 2006. Post-convection spreading phase in the Northwestern Mediterranean Sea. *Deep-Sea Research I* 53, 869–893.

Trincardi, F., Verdicchio, G., Miserocchi, S., 2007. Seafloor evidence for the interaction between cascading and along-slope bottom water masses. *Journal of Geophysical Research* 112, F03011, doi:10.1029/2006JF000620.

Ulses, C., Estournel, C., Durrieu de Madron, X., Palanques, A., 2008a. Suspended sediment transport in the Gulf of Lions (NW Mediterranean): impact of extreme storms and floods. *Continental Shelf Research* 28, 2048-2070.

Ulses C., Estournel, C., Puig, P., Durrieu de Madron, X., Marsaleix, P., 2008b. Dense shelf water cascading in the northwestern Mediterranean during the cold winter 2005: Quantification of the export through the Gulf of Lion and Catalan margin. *Geophysical Research Letters* 35, L07610, doi:10.1029/2008GL033257.

Ulses, C., Estournel, C., Bonnin, J., Durrieu de Madron, X., Marsaleix, P., 2008c. Impact of storms and dense water cascading on shelf-slope exchanges in the Gulf of Lion (NW Mediterranean). *Journal of Geophysical Research* 113, C02010, doi:10.1029/2006JC003795

Walsh, J.P., Nittrouer, C.A., 1999. Observations of sediment flux to the Eel continental slope, northern California. *Marine Geology* 154, 55-68.

Wahlin, A.K., Darelius, E., Cenedese, C., Lane-Serff, G.F., 2008. Laboratory observations of enhanced entrainment in dense overflows in the presence of submarine canyons and ridges. *Deep-Sea Research I* 55, 737-750.

Xu, J.P., Noble, M.A., Rosenfeld, L.K., 2004. In-situ measurements of velocity structure within turbidity currents. *Geophysical Research Letters* 31 (9), L09311 1-4.

## FIGURE CAPTIONS

Figure 1. Location of the study area in the southwestern part of the Gulf of Lions (northwestern Mediterranean Sea). Crosses indicate the location of the moorings in the Lacaze-Duthiers Canyon (LDC), Cap de Creus Canyon (CCC) and its southern open slope (SOS) deployed from October 2005 to October 2006. Each mooring is labelled according to its location and bottom depth (i.e., CCC 1000 for the mooring in Cap de Creus Canyon at 1000 m depth). The triangle shows the location of the wave buoy off Sète.

Figure 2. Long-term time series of near-bottom (30 m above seabed) and mid-water (470 m above sea bed) temperature measured at 1000 m total water depth in the Lacaze-Duthiers Canyon since October 1993. The drops in the 1000 m depth temperature record (red) indicate the deep cascading events that occurred in 1999, 2005 and 2006 (arrows).

Figure 3. Time series of water discharge from selected rivers of the Gulf of Lions coming from the Massif Central (Aude), the Pyrenees (Têt), and the Alps (Rhône).

Figure 4. Time series of average surface heat flux, wind speed and significant wave height (measured off-shore of Sète and Perpignan) for the Gulf of Lions shelf from October 2005 to October 2006.

Figure 5. Time series of near-bottom temperature and current speed measured at the mooring sites from October 2005 to October 2006.

Figure 6. Polar diagrams of near-bottom current speed at the mooring sites from October 2005 to October 2005.

Figure 7. Progressive vector plot of the currents measured at the mooring sites. In red the cascading season from 19 December 2005 to 30 April 2006; in Black from 16 October 2005 to 19 December 2005 and from 1 May to 25 October 2006. Crosses represent time periods of 30 days.

Figure 8. Time series of near-bottom SSC measured at the mooring sites from October 2005 to October 2006.

Figure 9. Cumulated suspended sediment fluxes estimated at the mooring sites from October 2005 to October 2006.

Figure 10. Average suspended sediment transport vectors in the study area for the 2006 cascading season (January-April).

Figure 11. Time series of near-bottom temperature, current and suspended sediment concentration measured at the Cap de Creus Canyon and southern open slope mooring sites during the first deep cascading pulse in early January 2006. Note changes of scale in current speed of CCC 1500, CCC 1990, SOS 1900 and in temperature and SSC at CCC 1900 and SOS 1900.

Figure 12. Time series of significant wave height, Têt River discharge and near-bottom temperature, current and suspended sediment concentration measured at the mooring sites

affected by the late January 2006 deep cascading pulse.

Figure 13. Time series of the near-bottom temperature, current and suspended sediment concentration measured at the Cap de Creus Canyon and southern open slope mooring sites during the March-April deep cascading pulses. Note changes of scale in SSC and temperature at CCC 1900 and SOS 1900.

Figure 14. Plots of SSC vs temperature, current direction and current speed and of current speed vs temperature for the deepest sites (CCC1900 and SOS 1900). Note the increase in SSC and current speed with temperature as a consequence of open sea convection.

Figure 1

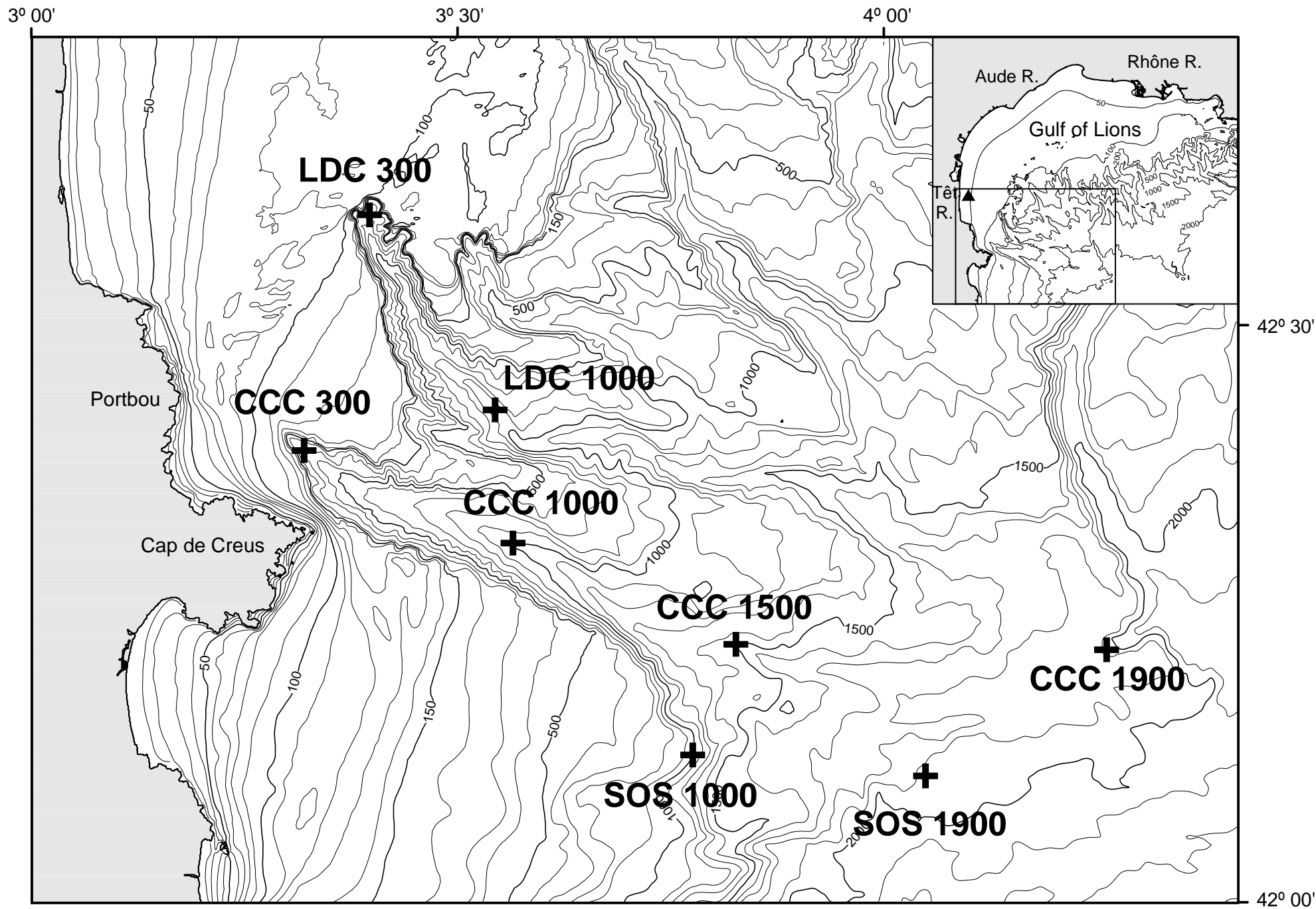


Figure 2

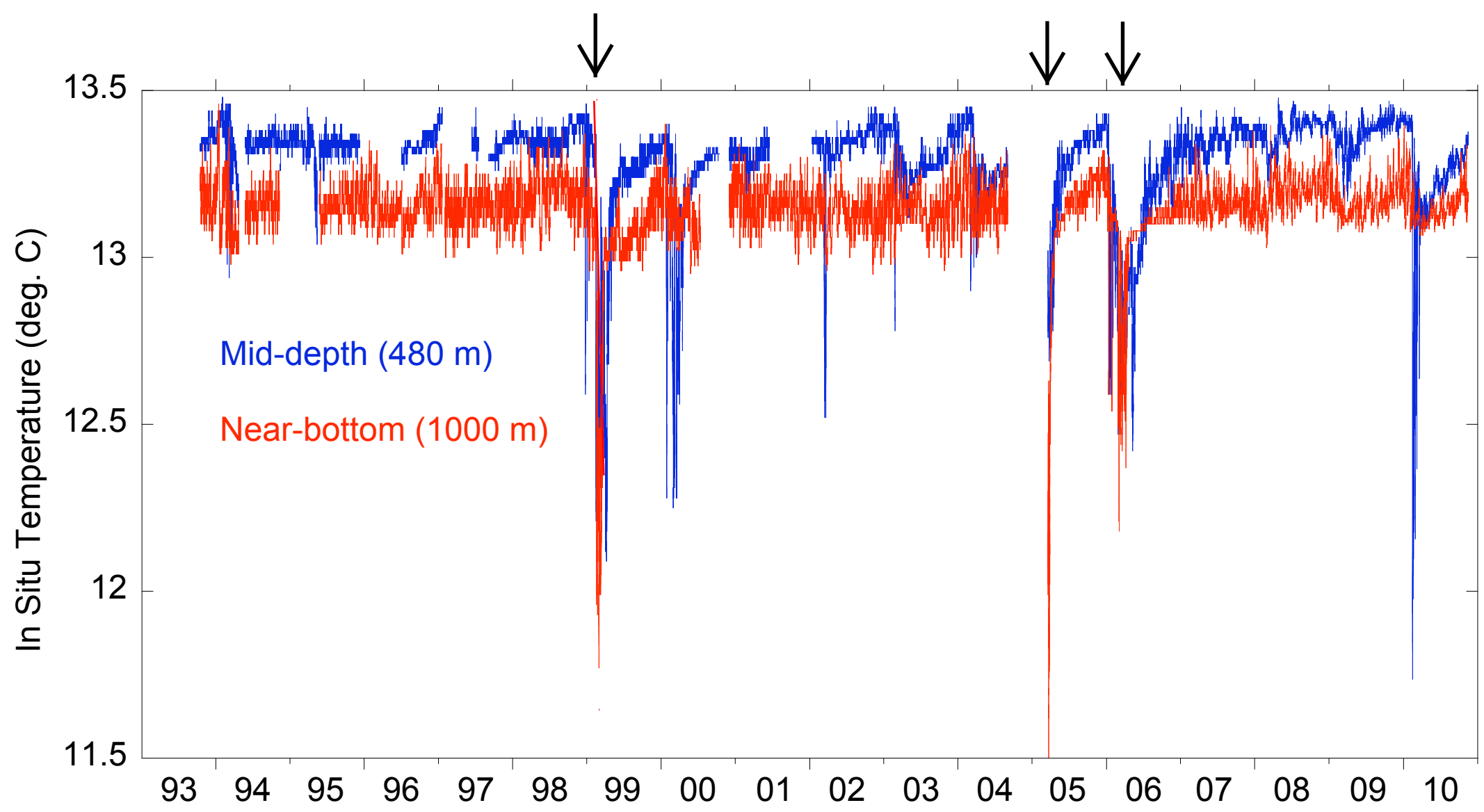


Figure 3

# River discharges

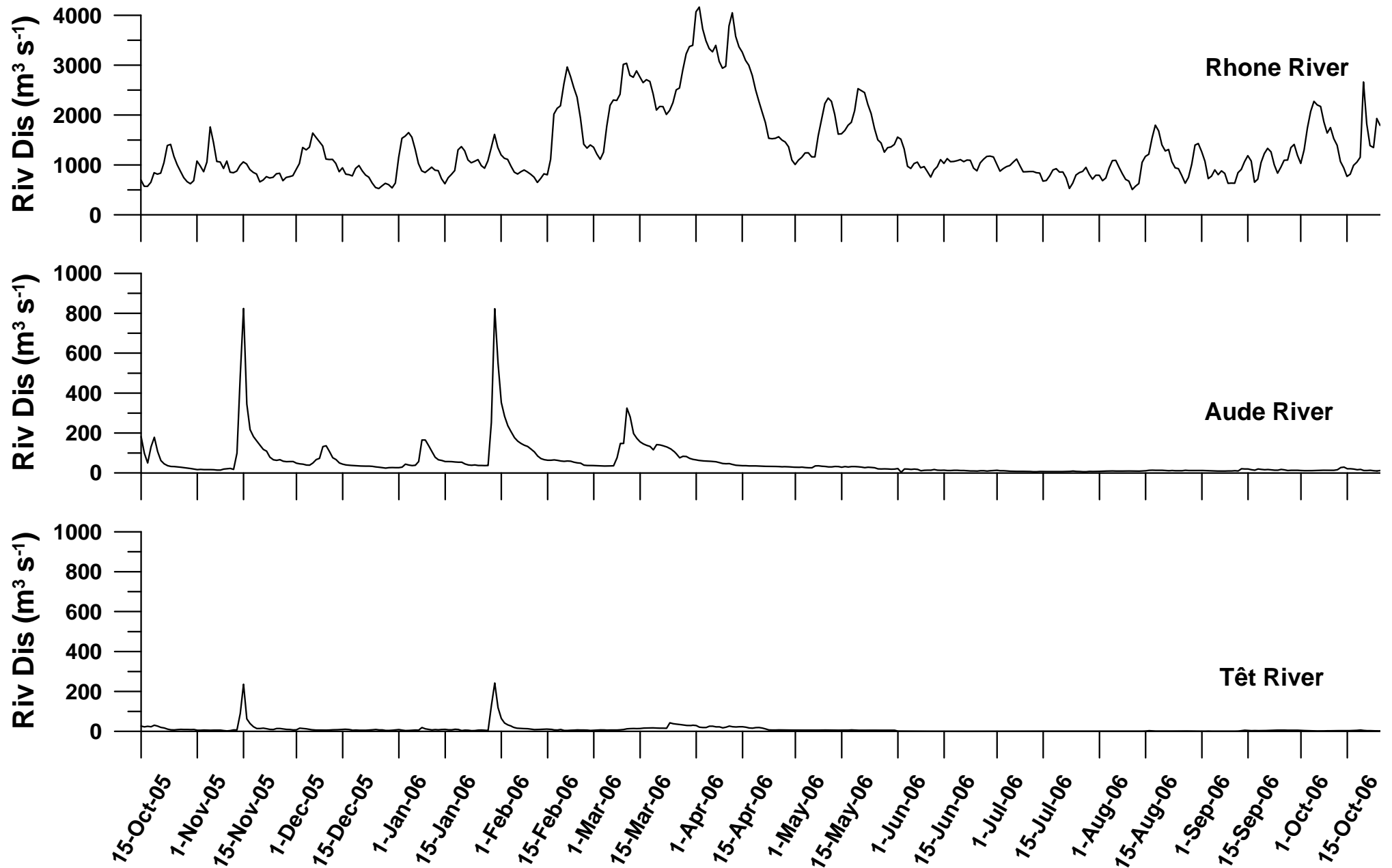


Figure 4

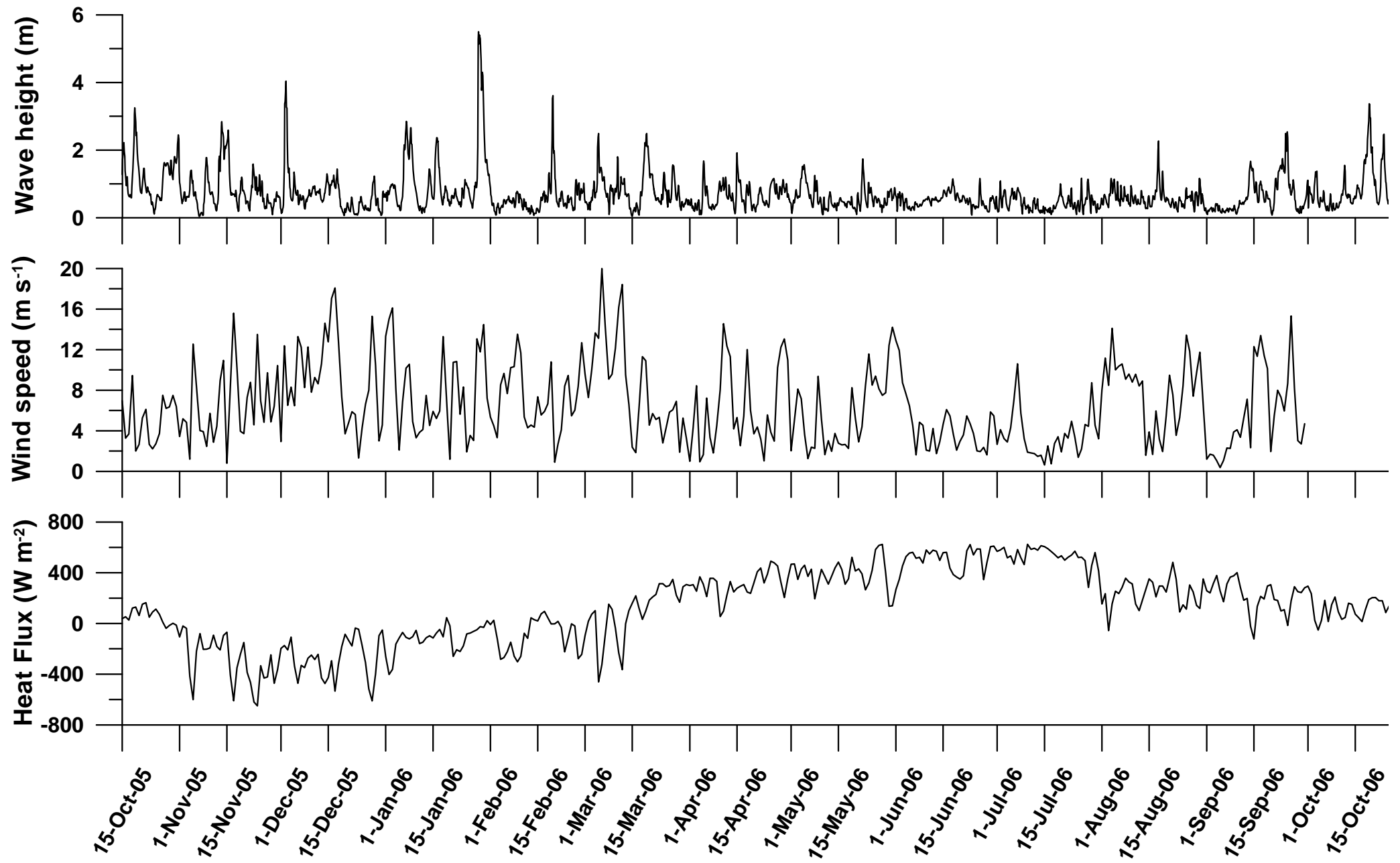
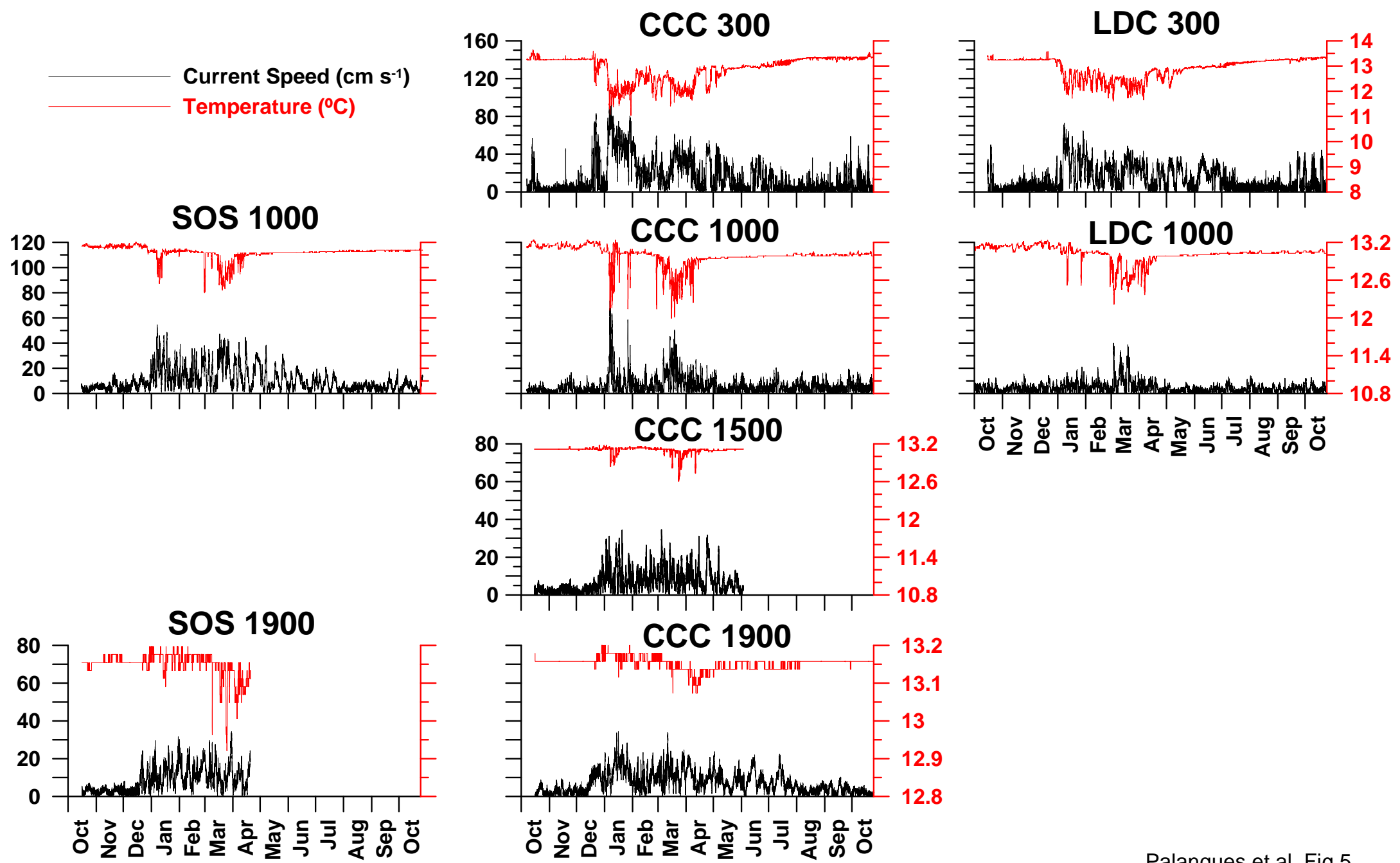


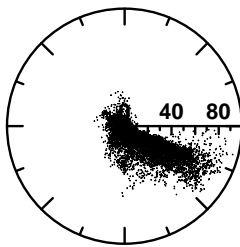
Figure 5



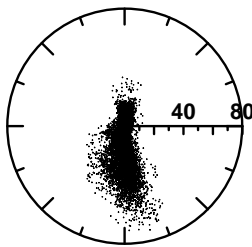
Palanques et al. Fig 5

Figure 6

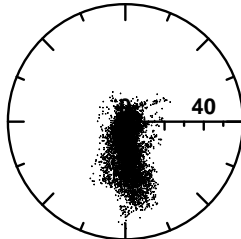
**CCC 300**



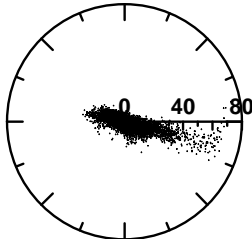
**LDC 300**



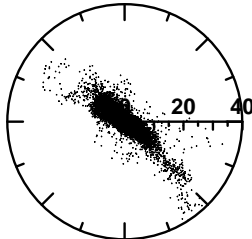
**SOS 1000**



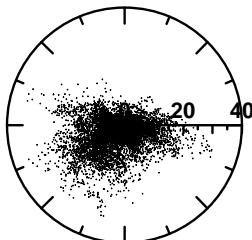
**CCC 1000**



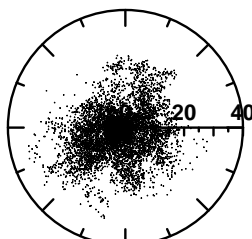
**LDC 1000**



**CCC 1500**



**SOS 1900**



**CCC 1900**

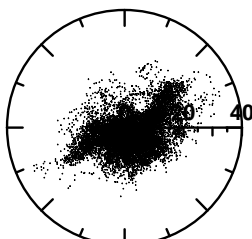


Figure 7

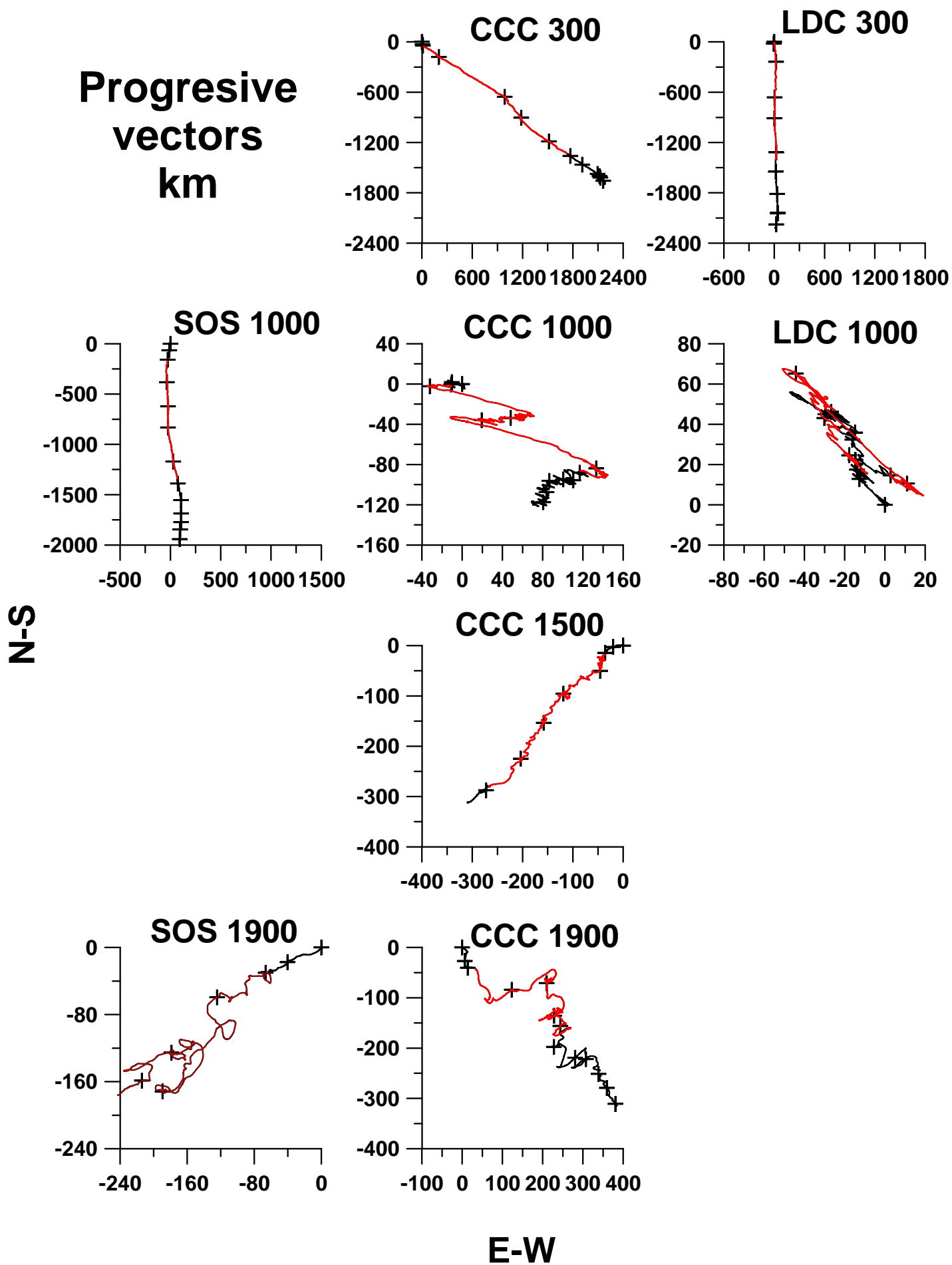


Figure 8

# Near-bottom turbidity (mg l<sup>-1</sup>)

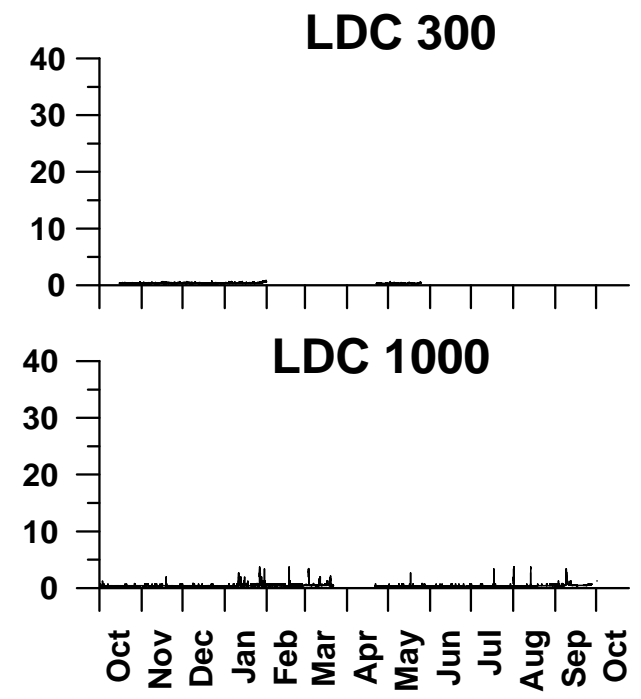
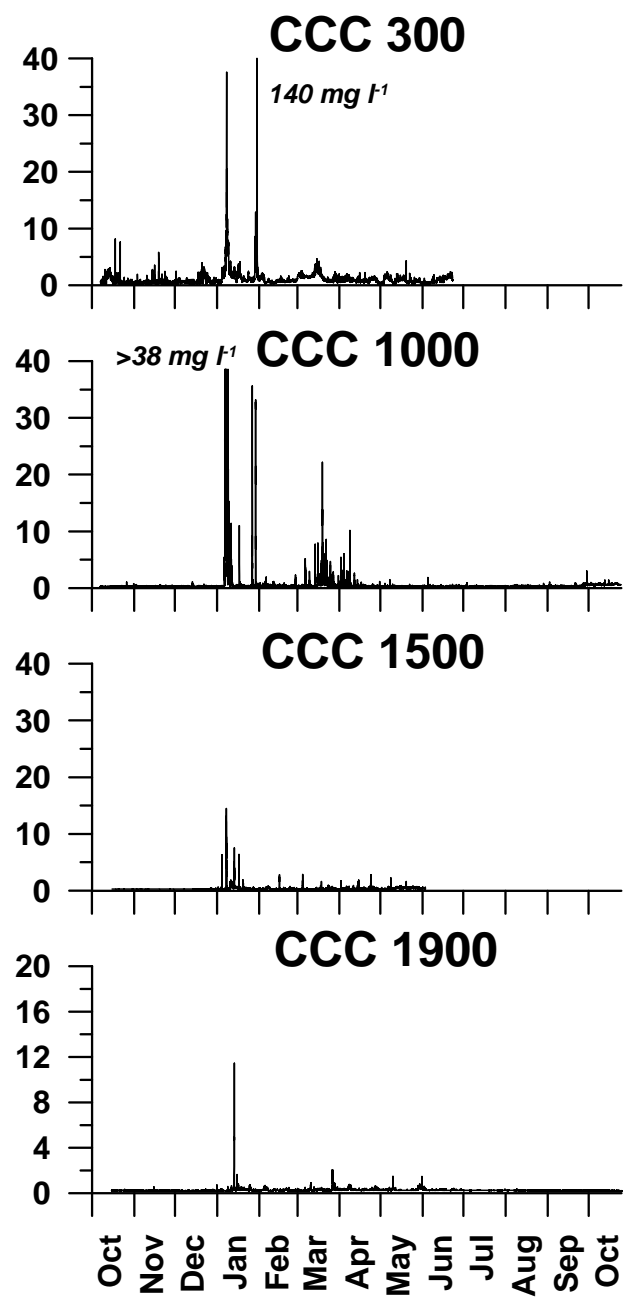
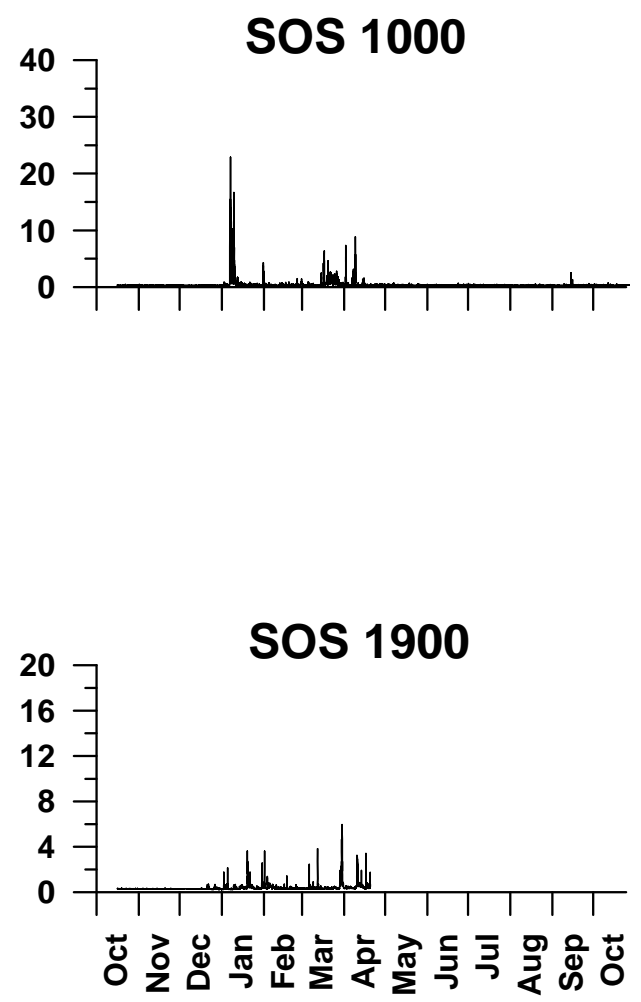
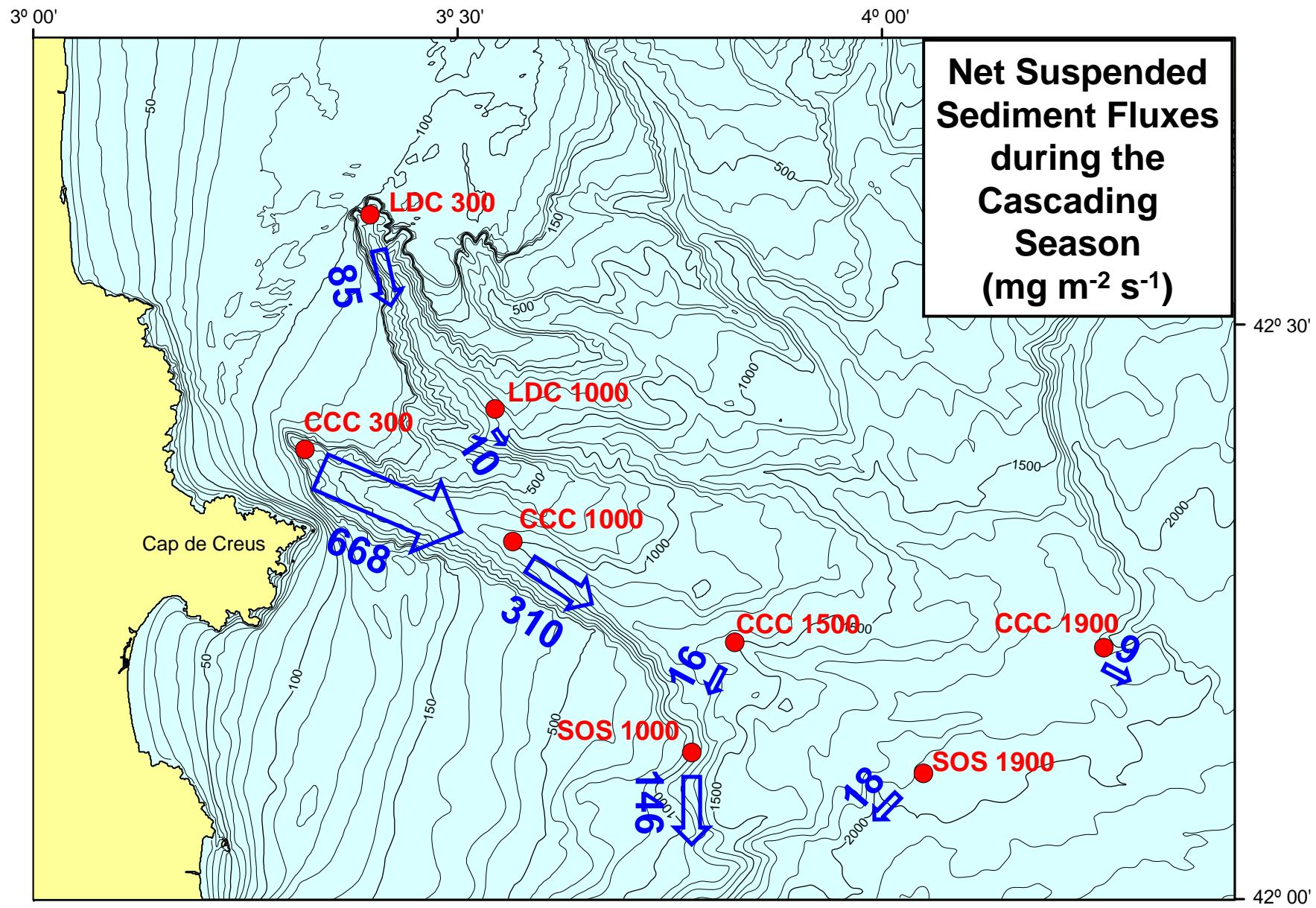




Figure 10



Palanques et al. Fig. 10

Figure 11

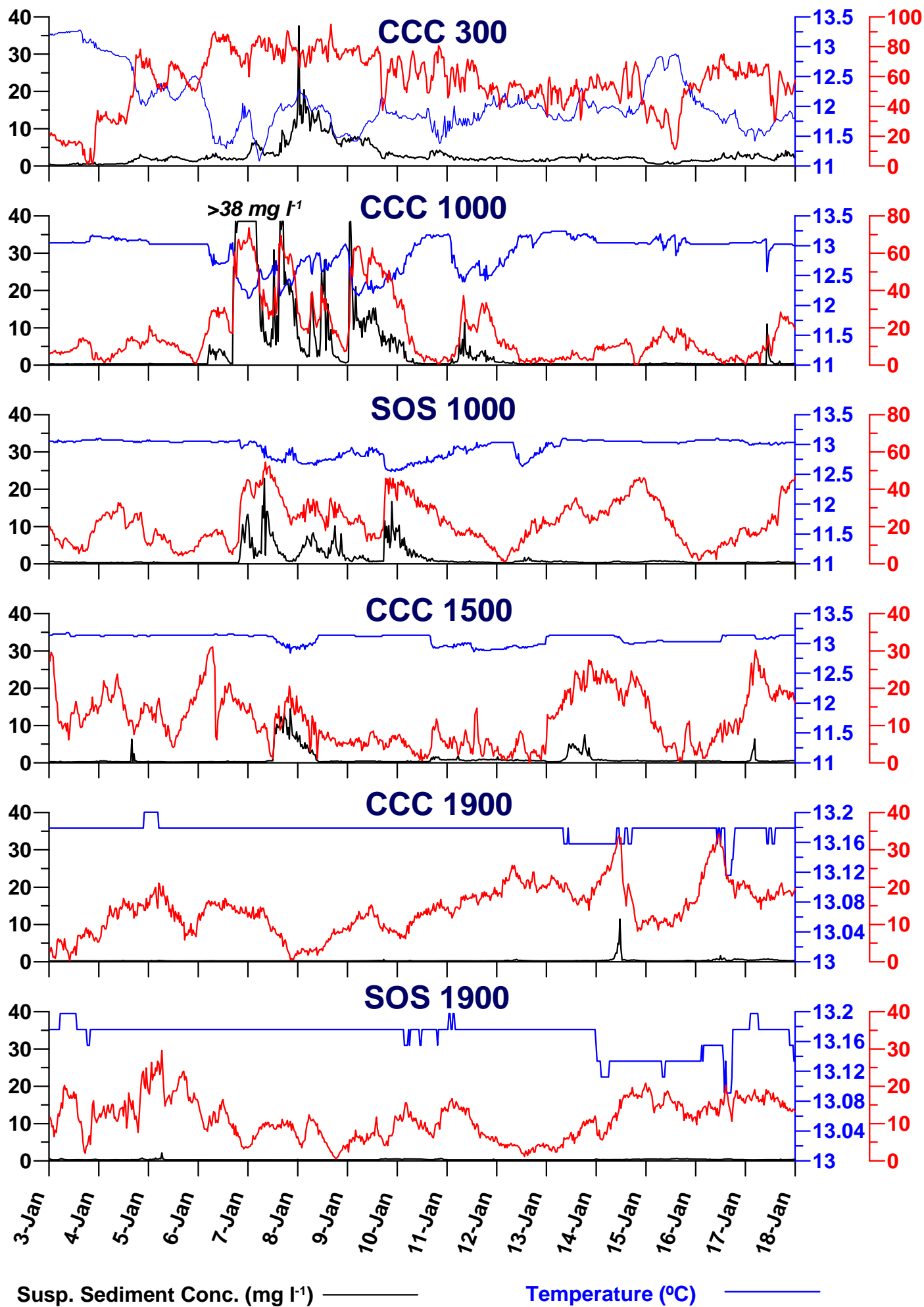


Figure 12

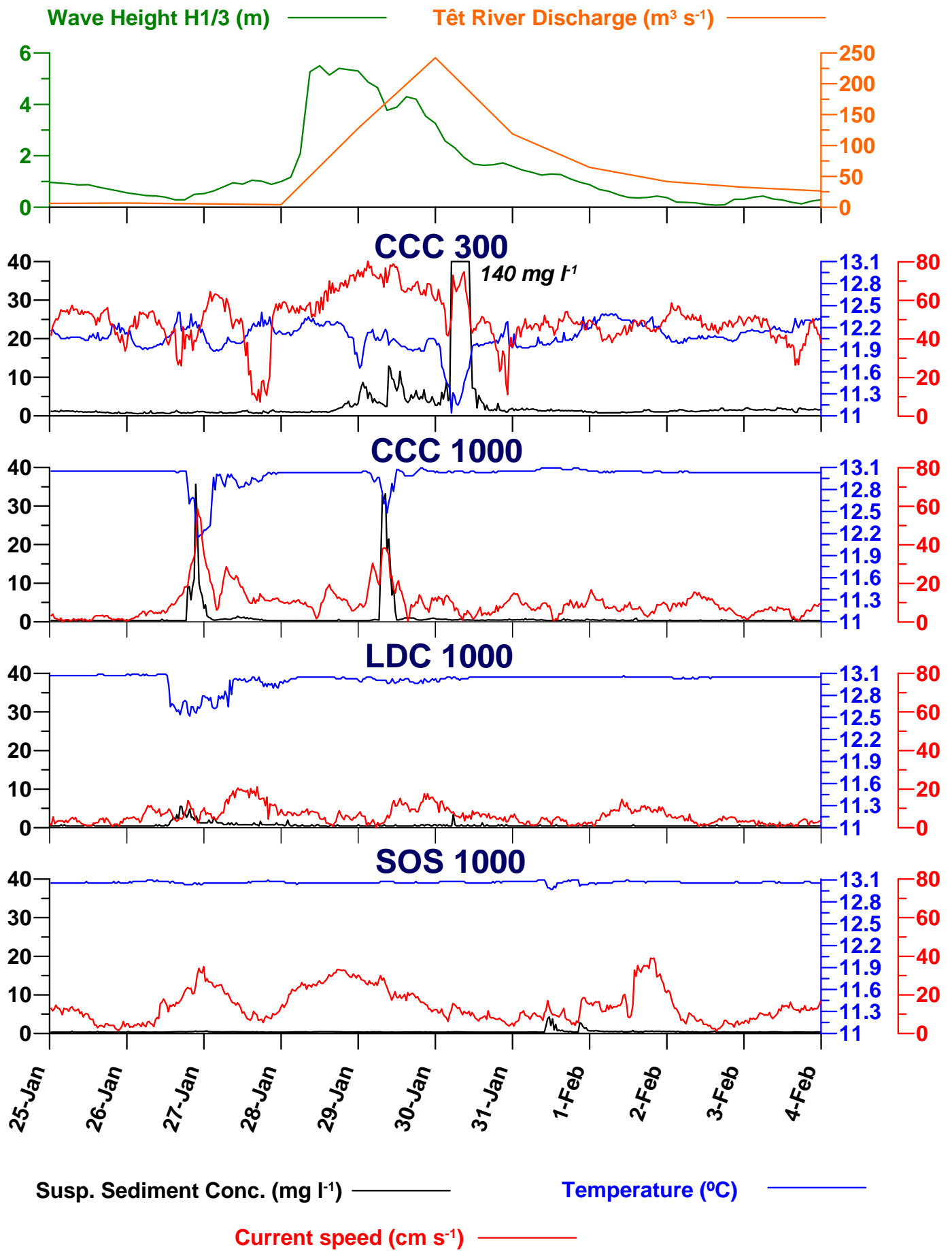


Figure 13

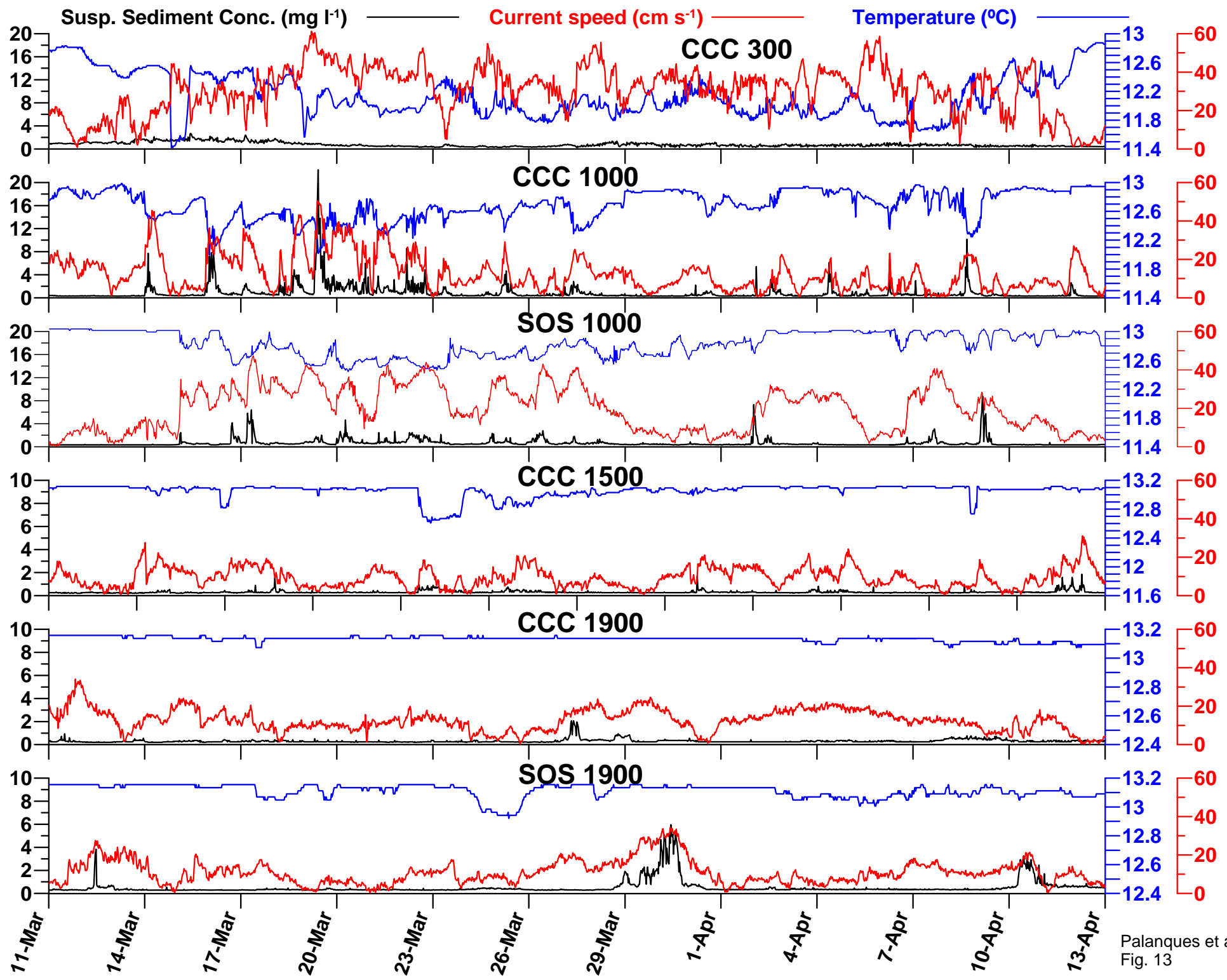


Figure 14

